

Freeform fabrication and characterization of Zn-air batteries

Evan Malone, Megan Berry and Hod Lipson

Mechanical and Aerospace Engineering, Cornell University, Ithaca, New York, USA

Abstract

Purpose – The paper's aim is to show the development of materials and methods which allow freeform fabrication of macroscopic Zn-air electrochemical batteries. Freedom of geometric design may allow for new possibilities in performance optimization.

Design/methodology/approach – The authors have formulated battery materials which are compatible with solid freeform fabrication (SFF) while retaining electrochemical functionality. Using SFF processes, they have fabricated six Zn-air cylindrical batteries and quantitatively characterized them and comparable commercial batteries. They analyze their performance in light of models from the literature and they also present SFF of a flexible two-cell battery of unusual geometry.

Findings – Under continuous discharge to 0.25 V/cell with a 100 Ω load, the cylindrical cells have a specific energy and power density in the range of 40-70 J/g and 0.4-1 mW/cm², respectively, with a mass range of 8-18 g. The commercial Zn-air button cells tested produce 30-750 J/g and 7-9 mW/cm² under the same conditions, and have a mass range of 0.2-2 g. The two-cell, flexible Zn-air battery produces a nominal 2.8 V, open-circuit.

Research limitations/implications – The freeform-fabricated batteries have ~10 percent of the normalized performance of the commercial batteries. High-internal contact resistance, loss of electrolyte through evaporation, and inferior catalyst reagent quality are possible causes of inferior performance. Complicated material preparation and battery fabrication processes have limited the number of batteries fabricated and characterized, limiting the statistical significance of the results.

Practical implications – Performance enhancement will be necessary before the packaging efficiency and design freedom provided by freeform-fabricated batteries will be of practical value.

Originality/value – The paper demonstrates a multi-material SFF system, material formulations, and fabrication methods which together allow the fabrication of complete functional Zn-air batteries. It provides the first quantitative characterization of completely freeform-fabricated Zn-air batteries and comparison to objective standards, and shows that highly unusual, functional battery designs incorporating flexibility, multiple cells, and unusual geometry may be freeform fabricated.

Keywords Electric cells, Design

Paper type Research paper

Introduction

Current freeform fabrication technologies allow manufacturing of high quality, primarily mechanical parts from a single material including polymers, ceramics, and metals. As mechanical product quality and durability has improved, researchers have begun exploring the potential for this technology to fabricate products with other functionality – active, multi-material components, such as sensors, actuators, amplifiers and logic gates, and power storage and generation units. We believe this trend will eventually lead toward freeform fabrication systems capable of producing complete integrated functional devices (Lipson, 2005). The ability to co-fabricate multi-material active devices directly from raw materials, combined with the ability to fabricate complex structures, will allow exploration of new system designs that take advantage of tight packaging, complex

device geometries and novel modes of form-function integration, including those previously observed only in biological organisms. Applications include novel biomimetic robotic architectures (Lipson and Pollack, 2000; Malone and Lipson, 2004), unmanned aerial/space vehicles (Mosher and Stucker, 2004), individually customized wearable devices (Weiss and Prinz, 1998), and more.

In prior work (Malone *et al.*, 2004), we presented the first freeform fabrication of a complete, functional, macroscopic zinc-air battery. These first devices produced were fragile and operated only briefly. We have since made improvements to our freeform fabrication system, battery designs, and material formulations, which have enabled us to produce Zn-air batteries robust enough for quantitative characterization. Here, we present these advancements, freeform fabrication of six complete Zn-air batteries of conventional “button” geometry, and test results for these and for comparable, commercially produced, Zn-air batteries. Analysis of the resulting data in light of the theoretical model of Mao and

The current issue and full text archive of this journal is available at www.emeraldinsight.com/1355-2546.htm



Rapid Prototyping Journal
14/3 (2008) 128–140
© Emerald Group Publishing Limited [ISSN 1355-2546]
[DOI 10.1108/13552540810877987]

This work was supported in part by the Learning Initiatives for Future Engineers student research grant program at Cornell University.

Received: 30 June 2006
Revised: 7 October 2007
Accepted: 9 January 2007

White (1992) allows us to identify likely performance bottlenecks and to identify approaches to improving the performance of the freeform-fabricated devices. As a demonstration of the future potential of this approach to fabricating batteries, we also present a prototype of a more complex battery design: a flexible, two-cell zinc-air battery with an unusual geometry.

In a typical application of commercially produced batteries (for instance, a laptop computer battery), multi-cell packs are made of connected cylindrical single-cell batteries in a rectangular package, resulting in wasted volume within the package. For a single layer of N cells of diameter d and length l packed tangent to each other, the exterior volume of the cells is $\pi Nd^2 l/4$, while the interior volume of the rectangular package is $Nd^2 l$, resulting in at most $\pi/4 \sim 79$ per cent of the package volume occupied with active material. For this reason, we believe that if either the power density or the energy density (or both) of freeform-fabricated batteries can be brought within roughly 20 per cent of that of commercial batteries, the design freedom afforded by solid freeform fabrication (SFF) will begin to outweigh the performance deficit, and freeform-fabricated batteries will begin to be of interest to industrial designers, and for wearable devices, unmanned aerial vehicles, and other highly geometry-constrained applications. Freeform methods will allow the fabrication of batteries packaged to match almost arbitrary cavities, containing the desired number and configuration of cells and filling far more of the available volume with active material than would be possible using arrangements of commercially produced cells.

Background

Experimentation with multi-material freeform fabrication of functional objects has been ongoing throughout the last decade. Weiss *et al.* (1997) were among the first to explore multi-material deposition and combined it with CNC machining and embedding of components into what they dub “Shape Deposition Manufacturing” (SDM). Functional and/or multi-material applications of SDM include copper-steel tooling, sensors embedded in metal objects, and novel packaging for wearable computers (Weiss *et al.*, 1997). The laser-controlled gas-phase “Selective Area Laser Deposition” process has been used to produce and embed complete functional Si/SiC thermocouples within ceramic objects (Lianchan and Shaw, 1999). Laser sintering/melting of selectively deposited slurries has been used to create multi-material dental prostheses (Wang *et al.*, 2004). Selective deposition of multiple powders followed by laser sintering has been used to produce components of combustion devices and electronics, including partial batteries (Kumar and Das, 2004; Kumar *et al.*, 2004). The laser-driven direct-write process MAPLE-DW, has been used to create a very wide variety of functional, multi-material products, including capacitors, conductors, partial batteries, and bio- and living-material structures (Auyeung *et al.*, 2000; Chrisey *et al.*, 2000; Wu *et al.*, 2003). Multi-material ink-jet deposition has been used to create electrical conductors and passive electronics (Chen *et al.*, 2003; Bidoki *et al.*, 2007), organic polymer transistors (Paul *et al.*, 2003), complete thermal actuators and partial electrostatic actuators (Fuller *et al.*, 2002), and biomaterial and living structures (Mironov *et al.*, 2003). Our work has employed syringe deposition and fused deposition within the

same system to fabricate structures, conductive wiring, and complete batteries (Malone *et al.*, 2004), electroactive polymer actuators (Malone and Lipson, 2006), organic polymer transistors (Havener *et al.*, 2007), and bio- and living-materials (Cohen *et al.*, 2006). Other groups are exploring multi-material stereolithography for tissue engineering (Arcaute *et al.*, 2006), and combining it with syringe deposition and component embedding to create electromechanical devices (Palmer *et al.*, 2006).

Higher levels of integration and hybridization in microelectronic devices, and the growing range of applications for MEMS devices in micro-spacecraft and distributed sensor systems have motivated research into methods of fabricating micro-batteries which are compatible with lithographic microelectronics manufacturing techniques. Sputtering and lithographic techniques (Neudecker *et al.*, 1999; Bates *et al.*, 2000; West *et al.*, 2002) have yielded complete and excellent thin film lithium batteries, but these techniques require the use of lithographic masks, and/or etching and/or high-temperature annealing, non-freeform/non-additive processes which restrict design freedom and integration with other fabrication processes. Additive “direct-write” processes have been used to produce components of both alkaline (Arnold *et al.*, 2004) and lithium-ion (Wartena *et al.*, 2004; Pique *et al.*, 2006) electrochemical batteries at the microscale suitable for integration with MEMS and microelectronics, but fabrication of complete batteries (including packaging, terminals and separator) entirely via direct-write has yet to be demonstrated. Interest in flexible batteries is rising for embedded applications in smart cards and RFID (Akashi *et al.*, 2002), and PowerPaper Ltd (2005) is manufacturing thin, flexible, alkaline cells through a lamination process.

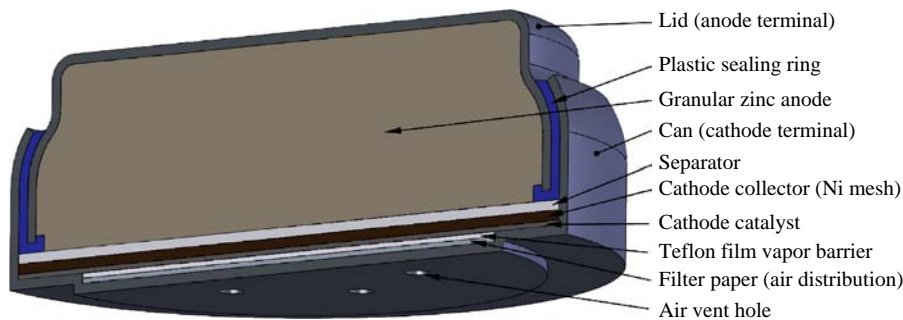
None of the aforementioned directly addresses the goal of our present research, namely achieving freeform fabrication of complete, macroscopic batteries with performance that rivals that of commercially produced batteries. As this goal is a non-traditional application of SFF, the reader is referred to Linden and Reddy (2002, Chapter 1) for background material on electrochemical batteries. Our reported performance results are calculated according to the definitions and theory provided there.

Experimental

The primary active materials of Zn-air cells (Figure 1) are a bound granular zinc anode, a powdered metal oxide cathode catalyst material, and a liquid or gelled basic (alkaline) electrolyte. Commercial Zn-air batteries typically also include a paper air-diffusion layer, a porous PTFE vapor barrier, a cellulose separator layer, and a nickel-mesh cathode collector, none of which are readily produced via SFF. During manufacturing, all of these materials are compressed tightly into a vented can and lid typically made of stainless steel.

The main challenge in freeform fabrication of batteries is finding selectively depositable material formulations which allow the fabrication of all essential components of a battery without compromising the performance of the finished device. The coupling between material formulation, material suitability for SFF processes, and fabricated device performance makes the development process very laborious. We therefore have focused the present work on making improvements to the most fundamental components of the battery – namely the Zn anode, separator, cathode catalyst, anode/cathode terminals, and casing. We consider the air-diffusion layer, vapor barrier, and

Figure 1 Cross section view of commercial Zn-air button battery



Source: Corrosion Doctors (2008)

cathode collector to be performance enhancing, but non-essential, and relegate them to future work.

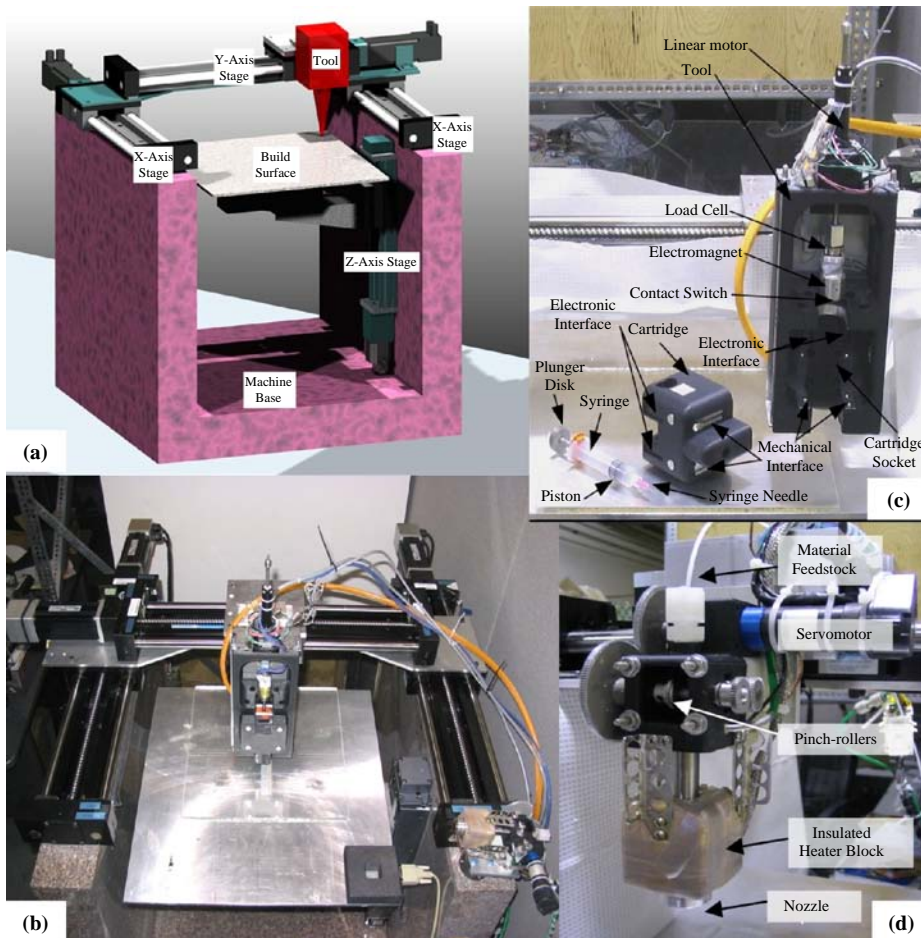
Freeform fabrication system

Our multi-material freeform fabrication research platform (Figure 2) consists of a three-axis Cartesian gantry robot, two changeable material-deposition tools, and a software application which processes assemblies of STL files into a multi-material manufacturing plan and executes the plan on the system hardware. Since our prior work with Zn-air

batteries (Malone *et al.*, 2004), we have reengineered both tools and improved the software to enhance deposition control, speed up changes of material, and simplify manufacturing of complex multi-material objects.

The *xy*-axis gantry moves the mounted tool along planned deposition paths, while the *z*-axis table moves downward to accommodate deposited material layers (Figure 2(a) and (b)). One tool (Figure 2(c)) employs syringe-deposition (robocasting) to deposit streams (roads) of material 250–1,500 μm in diameter, depending on material properties and

Figure 2 Multi-material SFF research platform: (a) CAD rendering of the Cartesian gantry positioning system; (b) photograph of actual system with syringe-deposition tool mounted; (c) components of syringe-deposition tool; (d) components of molten-extrusion tool



resolution/fabrication speed tradeoff. It is compatible with an enormous range of liquid, gel, or paste materials, and employs a linear stepper motor to achieve volumetric dispensing, at up to 1.1 MPa (160 psi). We have redesigned it to dispense from 10 ml disposable syringes mounted in easily changeable cartridges in order to facilitate rapid material changes. The second tool (Figure 2(d)), not employed in the present work, employs a molten-extrusion (FDM[®]) process, which entails feeding thermoplastic or low-melting point eutectic alloy feedstock in wire-form into a heated nozzle. This tool extrudes a fine strand (typically 150–200 μm diameter) of molten material which quickly solidifies, and now has active feedstock cooling, an optimized pinch roller tooth design, and a modular, finger-safe heating block. Tools are mounted to the *xy* gantry via a pneumatically-actuated robotic tool changer, which allows quick and accurate exchanges of tools.

We have created a custom computer-aided manufacturing (CAM) application which imports individual or assemblies of tessellated geometry (polyhedra) as STL files, generates hardware executable manufacturing plans, and controls their execution on the fabrication hardware. The system operator uses a graphical user interface (GUI) to specify with which material/tool combination each polyhedron should be fabricated. The toolpath planning consists of slicing each polyhedron according to the road thickness associated with its particular material/tool combination, offsetting resulting boundary polygons by 1/2 of the road width for the material/tool, and filling enclosed areas with raster (hatch) paths. Slices (containing paths) are then sorted by their height and executed, with the software prompting the operator to change the material and/or tool as required. Our hardware currently allows only one tool/material combination to be mounted at a time, and changes are manually executed, so time and labor become a significant factor for complex products, such as batteries.

To reduce the cost associated with tool/material switching, we have developed a fabrication process extension, dubbed “Backfill Deposition”, which allows overriding the layer height-ordering of the process plan to fabricate some parts of the structure before others. In practice, as geometry data describing component parts of a product such as a battery are imported into the fabrication system software, the operator may use the GUI to assign a sequential “fabrication priority” to each of the parts. Our SFF system will fabricate higher priority parts of an assembly to their full height prior to fabricating lower priority parts, in contrast to strict layered fabrication. This can reduce the number of tool changes in some cases from one per layer, down to one per STL file (or part). Additionally, this option facilitates fabrication of products which contain or are made from liquid materials – it allows the fabrication system to construct a container before filling it. For example, the case of a battery can be given a higher priority than the materials to be deposited into it and it will be completely fabricated to its full height before the deposition of the other materials begins.

Selection and formulation of materials

Our procedure for developing material formulations basically is to identify recommended formulations from the literature on Zn-air batteries, then to modify these to achieve rheological properties which allow reliable dispensing from a syringe with minimal loss of electrochemical functionality. We consider formulations to be syringe-dispensable when 10 ml

of material can be continuously dispensed from a syringe at 0.4 MPa (60 psi) without clogging. The electrochemical performance of material formulations which can be syringe dispensed is comparatively tested in handmade batteries of otherwise identical composition. Handmade batteries are constructed as shown in Figure 3.

Common elements are the ABS thermoplastic case, and anode and cathode terminals made of stainless steel mesh. Tests are made using 20 g of anode material, 1.5 g of cathode catalyst, and 1 g of separator material.

Separator

We selected the materials for the separator based on the research presented by Treger *et al.* (2000), who claim that a separator for an electrochemical cell can be formed *in situ* with a copolymer of polyvinyl alcohol (PVA) and polyvinyl acetate, or PVA alone. This technology proves particularly useful for application in freeform fabrication, as PVA can be deposited as a high-viscosity liquid conformal coating which will solidify to a thin film in the presence of potassium hydroxide present in the battery electrolyte.

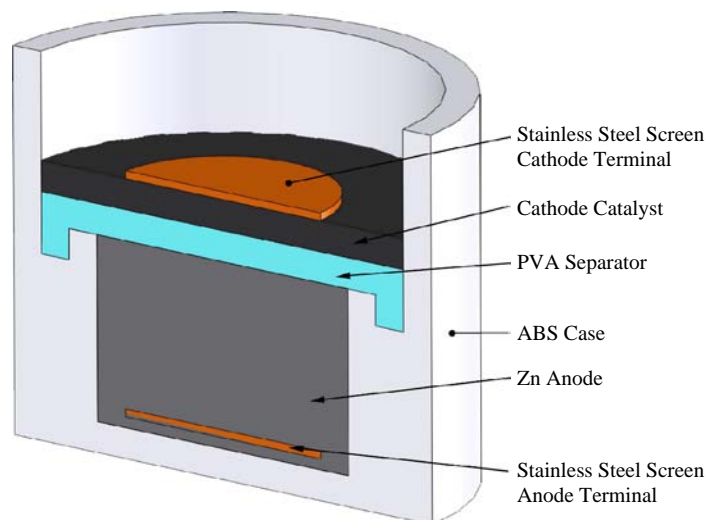
In initial experiments with the formulation in Treger *et al.* (2000), we found that the separator formed was quite rigid, and tended to curl at its edges, damaging our cells. The molecular weight distribution was changed slightly to favor a greater percentage of high-molecular weight PVA (Table I). This change allows the separator to remain permanently flexible while not adversely affecting the cell performance. The PVA is prepared by pre-mixing the dry materials in the appropriate ratio, and slowly adding them to 60°C water while stirring until fully dissolved. The solution is then ultrasonically degassed, and loaded into syringes for use.

Cathode catalyst

In commercial battery manufacturing, a dry cathode catalyst mixture is wetted with isopropanol, then mechanically kneaded, spread on a metal screen (which will act as the cathode current collector), and dried. Cathodes are then cut from the coated screen for installation into batteries. Chang and Chi (2001) present a catalyst formulation for metal air cells (Table II). We modify this dry mixture for freeform fabrication by adding gelling agent and electrolyte (Table III). The electrolyte serves the purpose of binding the dry mixture into a paste and the gelling agent prevents against phase separation during extrusion. The paste is mixed by hand and then allowed to stand for 12 h in order to fully hydrolyze.

Zinc anode

In formulating the zinc anode material, we balance rheology, reduction of hydrogen gas formation and electrochemical performance. Hydrogen gas formation prior to dispensing adversely affects dispensing control by making the material viscosity inhomogeneous; within a cell, it causes performance losses due to decreasing bulk density (hence conductivity) of the zinc anode and mechanical damage to the separator due to swelling of the anode. We manage rheology by selection of the Zn particle size distribution, and by formulating the material as a paste with electrolyte as the liquid component. The electrolyte concentration we employ is 8 M which is typically used in the art. The anode material is 40 wt%

Figure 3 Section view of design of handmade battery used for material formulation testing**Table I** PVA separator material formulations

Material	Original formulation (Treger, <i>et al.</i> 2000) (per cent)	Permanently flexible formulation (per cent)
PVA (M.W. 31-50 k)	11	10
PVA (M.W. 85-146 k)	3	4
PVA (M.W. 124-186 k)	1	2
Deionized water	84	84

Table II Catalyst dry mixture

Material	wt per cent
Manganese dioxide	20
Oxidized carbon black	77
PTFE 5 μm powder	3

Table III Catalyst paste formulation

Material	wt per cent
Catalyst dry mixture	75
Carbopol ultrez 21	7
8M aq. KOH	18

electrolyte, which falls under the recommendations given by Chang and Chi (2001) (35-40 per cent), Urry (1998) (25-55 per cent), and Bahary (1984) (30-40 per cent). The material is stabilized with a gelling agent, and both gas formation and electrochemical performance are affected by the selection of gelling agent, its concentration and the Zn particle size distribution.

We derived a list of candidate gelling agents from recommendations in the literature (Norteman, 1978; Graham and Goodman, 1980; Kerg, 1980; Bahary, 1984; Bennett *et al.*, 1996; Sumiya *et al.*, 2001), which focus on three categories: starch graft copolymers, carboxymethylcellulose, and

polyacrylic acid polymers. Graham and Goodman (1980) note that:

It has also been found that the use of (gelling agents of starch backbone and water soluble side chains) unexpectedly increases the practical discharge capacity of the anode while reducing the amount of cell gassing beyond that achieved through the use of previously known agents. Further, the internal resistance of the cell is not adversely increased.

Later research (Bennett *et al.*, 1996) claims:

[...] the gelling agent acts to push zinc particles into spaces among its swollen particles to promote contact among the zinc particles, or between the zinc particles and the negative electrode current collector.

Multiple gelling agents from each of these groups were tested. The best results were obtained using a starch-based polymer with acrylonitrile side chains, commercially available as Carbopol Ultrez 21 (BF Goodrich, Inc.).

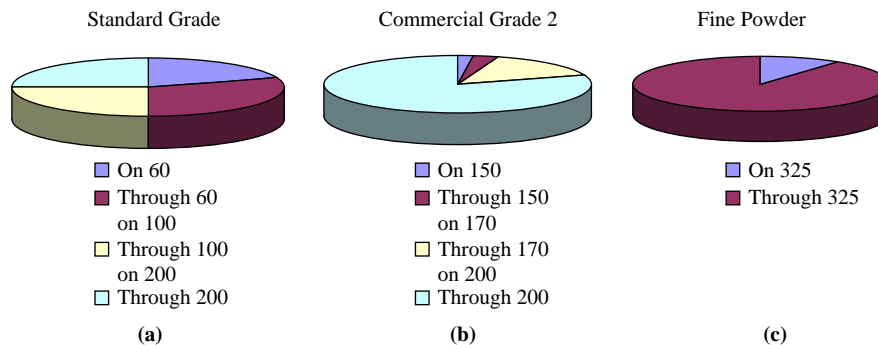
We performed a coarse search for an appropriate concentration of gelling agent, as shown in Table IV, and the outcome supports the claim that greater amounts of gelling agent increase cell capacity and power output. Gelling agent concentration in excess of 2 per cent causes near-solidification of the material, precluding extrusion. Therefore, a 2 per cent concentration was chosen as the best compromise between performance and rheology.

We explored several Zn particle size distributions (Figure 4) in formulations with 2 per cent concentration of Carbopol Ultrez 21. The literature (Durkot *et al.*, 1997; Chang and Chi, 2001; Oyama *et al.*, 2002) recommends particle sizes between 50 and 325 mesh. Durkot *et al.* (1997) state that the percentage of particles that pass through 200 mesh should be as much as

Table IV Performance of handmade cells with given amounts of gelling agent

Gelling agent (wt% of anode mat'l)	0 per cent	0.5 per cent	1 per cent	2 per cent
Energy output (J)	152.1	193.8	438.8	768.4
Average power output (mW)	0.53	0.54	1.43	2.25

Figure 4 Zinc particle size distributions: (a) standard grade zinc powder (Big River Zinc, Inc.); (b) commercial Grade 2 zinc powder (Big River Zinc, Inc.); (c) laboratory grade zinc powder (Sigma-Aldrich)



80 per cent, and claims that cells with high proportions of fine zinc powder have increased performance especially in high-drain usage due to a larger surface area of zinc in the anode. Oyama *et al.* (2002) state that both coarse and fine particles are needed, and that although increasing the amount of fine zinc particles improves discharge performance, it also increases generation of hydrogen gas through self-discharge.

Testing (Table V) revealed commercial Grade 2 (Big River Zinc, Inc.) to have dominant electrochemical performance with acceptable rheology and gas formation, making it the obvious choice. Fine Powder (Sigma-Aldrich) yielded superior rheology but excessive gas formation, and Standard Grade (Big River Zinc, Inc.) had the worst rheology and least gas formation.

The material is prepared for use by mixing the dry ingredients in the appropriate ratio, then adding the electrolyte and blending until uniform. The material requires 12 h to fully gel, after which it is remixed, and loaded into syringe barrels for use. Our formulation for the zinc anode is given in Table VI.

Case and terminal materials

We employ two additional materials in the fabrication of batteries. A room-temperature vulcanizing (RTV) silicone

Table V Performance of handmade cells versus type of zinc powder employed

Zinc type	Fine powder	Standard grade	Commercial Grade 2
Gelling agent (wt%)	2	2	2
Energy (J)	400.1	333.9	768.3
Ave. power (mW)	1.75	0.92	2.29
Continuous service (h)	62.7	100.2	94.4

Table VI Zinc anode material formulation

Material	Weight of zinc (per cent)	Weight of total (per cent)
Zinc Powder	100	70.4
8M aq. Potassium Hydroxide	40	28.2
Gelling Agent	2	1.4

(GE Silicone II, GE Silicones, Inc.) is used for the fabrication of the battery case and cap. This material is flexible, vulcanizes quickly (1–2 h), is chemically resistant and inert, self-supporting, and easily deposited with 250 μm resolution. The conductive terminals are produced using an RTV silicone filled with silver particles (SS-26, Silicone Solutions Inc.). This material is also chemically resistant and flexible, and bonds well to the silicone case to form a very robust conductor. The manufacturer claims an electrical resistivity of $5 \times 10^{-3} \Omega \text{ cm}$ for the material.

Fabrication experiments

The process of freeform fabricating a battery comprises the following steps: tuning deposition control parameters for each material, designing the battery model to be produced, and planning and executing the fabrication process. The deposition control parameters must be determined for each of the materials in a calibration process. This involves identifying a syringe tip with an appropriate form (tapered tips for viscous homogeneous materials, needles for multi-phase materials) and diameter (larger diameter tips for more viscous or more phase-separation prone materials) for each material. During formulation experiments, we typically identify the smallest diameter tip through which material can be reliably extruded, which also indicates the best achievable resolution with that material. Based on the selected tip, initial deposition parameters can be calculated, including the volumetric flow rate, and estimated road width and height. These and acceleration parameters are then iteratively tuned by commanding the system to deposit a test pattern with the material, measuring the pattern, and correcting the parameters until the deposited and designed pattern dimensions match. Our tip selection and tuned road dimensions for each of the materials used in this work are shown in Table VII.

Table VII Syringe tips and road dimensions for each material

Material	Tip ID (mm) and type	Road width (mm)	Road height (mm)
Silicone casing/cap	0.25 PE tapered	0.26	0.24
Anode/cathode conductor	1.37 SS needle	1.40	0.90
Zinc anode	0.84 SS needle	0.90	0.80
PVA separator	0.25 PE tapered	0.25	0.25
Cathode catalyst	0.51 SS needle	0.80	0.50

Designing a battery for freeform fabrication with our system is relatively simple, and any 3D design software which can export in STL format may be used, but there are a few technical details about the manufacturing process that the designer must bear in mind. Objects are sliced by the path-planning algorithm in layer thicknesses determined by the road height of the material assigned to the object. Thus, no paths will be generated for objects that are shorter than 1/2 the road height. Additionally, unless carefully designed, interfaces between different materials can result in layer-height mismatches because of discretization at different resolutions. Thus, the designer must bear in mind the material road height for each part of the battery, and design components to be of an integral number of layers. Additionally, deliberate alteration of the material deposition parameters after tuning may be used to provide another layer of control over the morphology of the material being deposited. For instance, by increasing the road width of the catalyst significantly (Table VII), a catalyst layer designed as a solid disk will instead be produced as an open mesh. We use this technique to enhance gas diffusion through the catalyst layer.

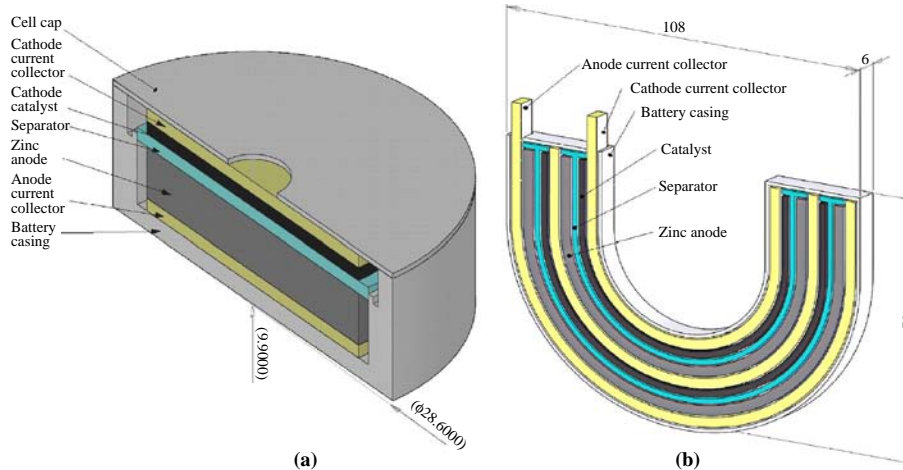
Figure 5(a) presents the design of the “SFF Basic” cylindrical battery that we have produced in three variants for performance comparison to commercially available “button” batteries. “SFF Basic” is 28.6 mm OD \times 10 mm H. The “SFF Half” variant design has a reduced diameter which results in a \sim 50 per cent smaller cross-sectional area. The “SFF Triple” variant has a 300 per cent enlarged cross-sectional area relative to the basic design. All three variants are designed to have the same mass of reactants.

In order to begin exploring the design freedom possible with freeform fabrication of batteries, we have also designed a two-cell (in series) battery with an unusual geometry. We chose a U-shape where the layers were organized horizontally instead of vertically to allow air flow to both catalyst layers. This parallel linear arrangement of materials, the thin silicone case, and our separator formulation should allow the battery to be flexible as well. The CAD model of the battery is shown in Figure 5(b), and has external dimensions of 110 \times 80 \times 5 mm.

Planning the fabrication process involves importing the STL files exported from the design application into our CAM application. As described previously, the user assigns a material to each model component imported and may optionally assign a fabrication priority. When fabricating one of the cylindrical battery variants, we set the battery case and the anode conductor to the same elevated priority, and all other materials are given the lowest priority. Upon execution, the case and anode conductor are deposited in a normal (non-backfill) layer-wise fashion (Figure 6(a)), which allows the anode conductor to extend through an opening in the wall of the case for ease of connection. The case is deposited up to its full height, and then the zinc anode layer and PVA separator layer are backfill deposited in succession (Figure 6(b)). At this point, fabrication pauses for 15 min in order to allow the PVA to be solidified by the potassium hydroxide electrolyte in the zinc anode material (Figure 6(c)). The PVA separator is thus much less likely to be damaged by the deposition of subsequent materials. The catalyst, cathode current conductor, and casing cap layers are then deposited without further delay, and the battery is complete (Figure 6(d)). In order to monitor the mass of active materials deposited, we fabricate each of the cylindrical batteries on a sheet of polyester film on a laboratory balance placed on the fabrication system build surface. Six cylindrical batteries were successfully fabricated for characterization – four “SFF Basic”, and one each of the “SFF Half” and “SFF Triple” variants. Fabrication times are 1.43 h for a “Half”, 1.25 h for a “Basic”, and 1.83 h for a “Triple”.

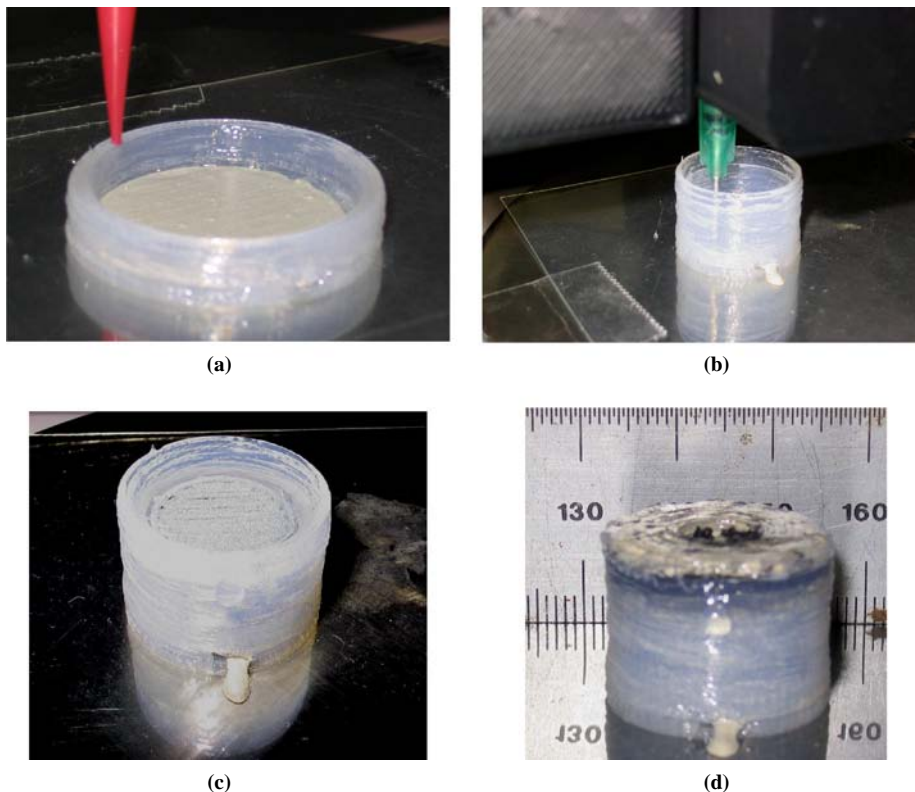
Planning of the “U” battery manufacturing process is complicated by the facts that the PVA material is of low-enough viscosity that it flows under gravity, and that the separators cannot be deposited as simple planar layers, regardless of the orientation of the battery during fabrication. Thus, we assign the separator layers the lowest priority, so that they are deposited after the anode and cathode, and the PVA will flow down between these. To minimize tool changes, each of the materials in the battery is given a separate priority: the case is given the highest priority, followed by the anode and cathode current conductors, then the anode, then the cathode catalyst, and finally the separator. The “U” battery requires roughly 4 h to be produced.

Figure 5 (a) CAD model of “SFF Basic” design cylindrical freeform-fabricated battery; cutaway showing components (inset), and exterior view revealing cathode conductor, catalyst, and separator; (b) CAD model of freeform “U” shape, two-cell battery



Note: Cap hidden for clarity

Figure 6 Freeform fabrication of a complete Zn-air battery: (a) the silicone case is being fabricated and the anode current collector has already been extruded; (b) backfill deposition of the zinc anode material into the case; (c) the PVA separator has been deposited atop the zinc anode, and fabrication is paused to allow solidification of the separator; (d) completed battery



Testing methods

A total of six cylindrical batteries were tested – four SFF Basic, and one each of the Half and Triple variants. We have also tested three different sizes of Zn-air button batteries produced by Renata SA of Switzerland (Renata, 2005) – the ZA 5 (eight tested), ZA 10 (four tested) and ZA 675 (four tested) under the same conditions to provide an objective reference standard. We test both the commercial and the freeform-fabricated batteries using a PC-based data acquisition (DAQ) system. Electrical contact is made to the freeform-fabricated batteries by piercing the anode and cathode current collectors with 32AWG copper wires which are clipped to the DAQ system test leads. The commercial button-cell batteries are pinched between isolated BeCu spring wire contacts. All batteries are first allowed to reach a stable open circuit voltage before we place a load of $100\ \Omega$ in the circuit. We use software to record the voltage across the load resistor at a sampling period of one minute. We cease collecting data when the cell voltage remains consistently below 0.25 V.

Results and discussion

Table VIII summarizes our test results for the commercial and freeform-fabricated batteries, and includes the design and operating condition recommendations of Mao and White (1992) for comparison and diagnosis. Figure 7 graphically shows key structural and performance parameters for commercial and freeform batteries. Discharge curves for both types are shown in Figure 8.

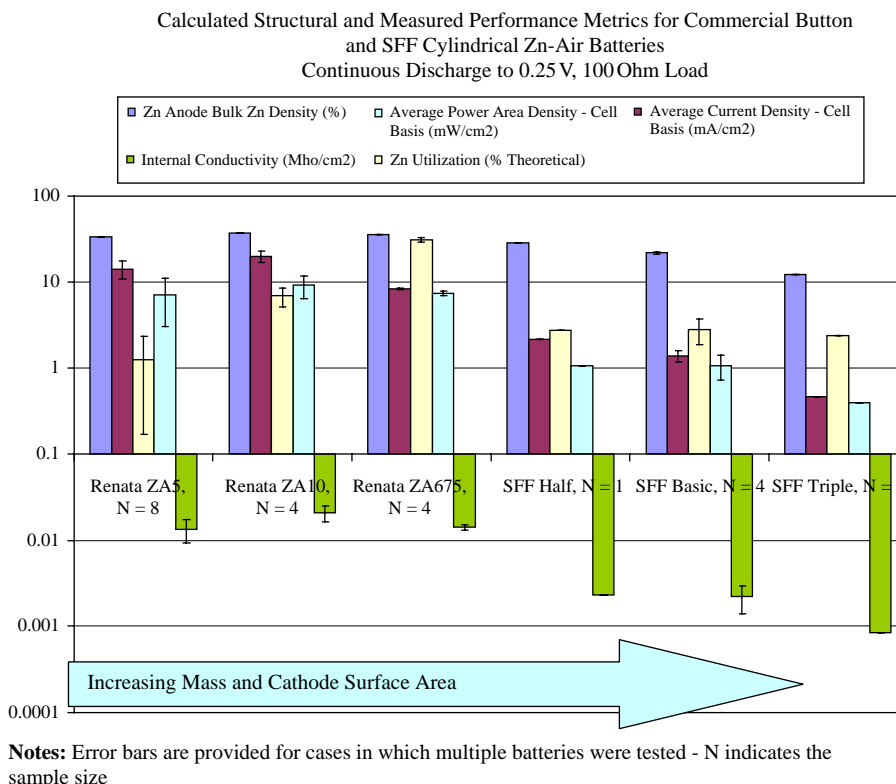
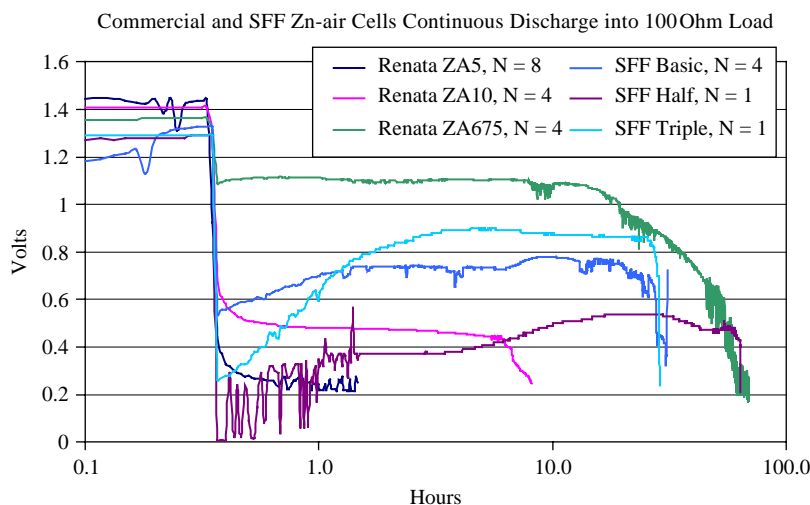
It can be immediately observed from Figure 7 that the performance of the freeform-fabricated batteries is an order of magnitude inferior to that of commercial button cells in most metrics, in particular power density. This suggests investigating causes for low-output voltage and low-current density in the freeform batteries. The loading condition in our tests is fairly demanding, and none of the batteries is operating at the nominal 1.2V expected for Zn-air (Table VIII), but there is not a substantial difference between the commercial and the freeform output voltages. In the case of current density, the commercial batteries are operating near, though below the $20\ \text{mA}/\text{cm}^2$ upper limit suggested by Mao and White (1992). The freeform batteries are a full order of magnitude below it, however. This suggests that high-internal resistance or low-electrochemical activity is responsible.

Figure 7 shows that conductivity of the freeform-fabricated cells is not consistent as the cross-sectional area of the cell varies – it actually decreases with increasing surface area, whereas it is roughly constant for the three sizes of commercial cells. This suggests that the bulk conductivity of some of our materials is low, or the contact resistance between materials is high – charge is not being collected and transported to the terminal connections effectively. The culprit is not obviously the Zn anode – the bulk densities of the freeform anodes are within a factor of two or three of those of the commercial cells (Table VIII and Figure 7). The cathode catalyst and/or the current collectors/terminals may be responsible.

Table VIII Specifications and performance for commercial button and SFF cylindrical Zn-air batteries

Battery	Mass (g)	Design cathode area (cm ²)	Design anode height (mm)	Zn anode density (per centage of bulk Zn)	Internal cond. (Mho/cm ²)	Average output voltage (V)	Average current density (mA/cm ²)	Average power density (mW/cm ²)	Specific energy (J/g Zn)	Spec. energy per cent theor.
Mao and White (1992)			$2 < d < 5$	26.91	0.01	1.20	20	12.00	1704	<35
Renata ZA5 (N = 8)	0.18	0.22	1.68	33.06	0.0135 ± 0.0042	0.27 ± 0.04	14.30 ± 3.47	7.08 ± 4.09	61.0 ± 52.9	1.25 ± 1.09
Renata ZA10 (N = 4)	0.34	0.22	2.88	36.92	0.0209 ± 0.0044	0.44 ± 0.07	19.85 ± 3.04	9.15 ± 2.62	334 ± 84.4	6.86 ± 1.73
Renata ZA675 (N = 4)	2.16	0.97	4.32	36.18	0.0142 ± 0.0096	0.81 ± 0.02	8.36 ± 0.24	7.40 ± 0.40	$1,510 \pm 98.1$	31.00 ± 2.02
SFF half (N = 1)	8.04	2.27	9.00	28.25	0.0023	0.49	2.14	1.05	132	2.73
SFF basic (N = 4)	10.13 ± 0.34	5.31	6.00	21.75 ± 0.66	0.0022 ± 0.0008	0.74 ± 0.11	1.39 ± 0.21	1.07 ± 0.34	136 ± 44.4	2.80 ± 0.91
SFF Triple (N = 1)	17.89	18.10	4.02	12.15	0.0008	0.85	0.47	0.40	117	2.39

Notes: N indicates sample size; standard deviations are given for averaged experimental data

Figure 7 Structure and performance comparison between several sizes of commercially manufactured Zn-air batteries and SFF Zn-air batteries**Figure 8** Discharge curve comparison between commercial Zn-air button and SFF Zn-air cylindrical batteries

Our catalyst layers are 2-3 mm thick, as compared to the ~ 0.5 mm thickness suggested by Mao and White (1992), and our catalyst formulation at present makes use of reagent grade MnO_2 , rather than the “electrolytic manganese dioxide” or chemically synthesized blend of $\text{MnO}_2/\text{Mn}_2\text{O}_3/\text{Mn}_3\text{O}_4$ recommended by Passaniti and Dopp (1994), Borbely and Molla (1990) and others. The excessive thickness of our catalyst may reduce the rate of air diffusion to the active (electrolyte) surface of the cell, and may also increase the electrical resistance between the active surface and the cathode current collector.

The commercial batteries are packaged in stainless steel cans which act as terminals, and include a metal mesh screen embedded within the cathode catalyst material to improve charge collection. Our SFF batteries use a silicone RTV filled with silver particles (Silicone Solutions, Inc., SS-26) as the anode and cathode current collectors/terminals because it is easy to dispense, and bonds well to the silicone RTV case greatly improving the robustness of the batteries. The bulk resistivity of the material is fairly high, however ($5 \times 10^{-3} \Omega\text{-cm}$ – compare with $7 \times 10^{-5} \Omega\text{-cm}$ for type 316 stainless steel), and our current freeform fabrication method results in

very little compression of layers – the materials simply rest against each other. In addition, in qualitative experiments we have found that it is quite difficult to make good electrical contact with the material – probably due to it comprising a conducting particulate phase in a highly insulating matrix.

The freeform-fabricated batteries are not achieving the 25–35 per cent Zn utilization which Linden and Reddy (2002) claim is typical for commercial batteries, and which the ZA 675 seems to achieve (Table VIII). Mao and White (1992) suggest several causes of reduced utilization. These include excessive Zn loading, excessive current density, and loss of electrolyte. Our data seem to indicate that both the Zn loading and the current density for our freeform-fabricated batteries are reasonable, and in fact below the levels suggested by Mao and White (1992), and below the levels calculated for the commercial batteries tested. In addition, the flat discharge curves for our batteries (Figure 8) support the notion that excessive current density is not the problem. One consequence of excessive discharge rate is rapid precipitation of ZnO within the anode due to the ZnO generation rate greatly exceeding its rate of dissolution and transport within the electrolyte. This results in electrical insulation – passivation – of the unreacted anode material from the electrolyte, a rapid decline in output voltage, and low utilization. This rapid decline in output voltage can be observed (Figure 8) for the Renata ZA 5 and ZA 10 which fail in less than 8 h (we are testing them with a 100 Ω load while the manufacturer's specifications are generated for 1,500 Ω loads). Our freeform-fabricated batteries maintain their flat discharge curves (Figure 8) for 30–60 h. This suggests that the loss of electrolyte solvent through evaporation may be causing the very low utilization. Additional support for this conclusion can be drawn from the fact that our battery with the smallest cross-section (SFF Half) has both the highest current density and the highest Zn utilization of all the SFF batteries. This is reasonable because while it has about the same mass of reactants as the other SFF batteries, the surface area exposed to the atmosphere is much smaller relative to the volume of reactants than is the case for the other SFF batteries. It seems likely that vent holes we provide in the battery cases are too large, and not sufficiently limiting the evaporation rate of electrolyte.

As a demonstration of potential customization of geometry and function, the freeform fabrication of the “U” shaped battery was partially successful, and the finished device (Figure 9(a)) looks grossly similar to the design (Figure 5(b)).

Closer inspection revealed some regions where the cathode catalyst and anode material are not clearly separated by PVA. During testing, the device generated 2.5 V, open-circuit, clearly indicating the functioning of both (1.4 V) cells in the two-cell configuration. During testing with a 100 Ω load, the output potential only remained above 0.5 V (0.25 V/cell) for 5.1 h. In this time, the battery generated about 20 J/g, and upon removal of the load, the open-circuit voltage only returned to 1.4 V. The reduced open-circuit voltage is possibly a result of flaws in the separator layers which may have allowed some internal shorting. In any case, the battery maintains the 1.4 V open circuit output even when twisted and bent as shown in Figure 9(b).

Future work

We have identified five areas of future work relevant to improving the performance and customizability of our freeform-fabricated batteries. Firstly, we will examine the bulk resistivity of the current collector and anode materials, and the sensitivity of contact resistance between these materials to compression. While achieving compression via freeform fabrication is an open problem, we have already identified candidate alternative collector/terminal materials, including commercial silver-ink and PVA or polyvinyl acetate filled with silver and/or nickel flake. Secondly, the effect of cathode catalytic activity will be examined by comparing our existing catalyst to one formulated with materials produced specifically for battery application. Thirdly, the effect of the thickness of the catalyst layer on performance will be studied. Fourthly, we will examine the evaporative loss of electrolyte as a cause of low-zinc utilization by tracking the change in mass of freeform-fabricated batteries as they discharge. Should there prove to be a significant correlation between mass loss and performance, we can easily modify our designs and fabricate batteries with much smaller vents, and can also investigate the use of a vapor-barrier material. Finally, new design “tricks” and manufacturing sequences will be developed in order to increase the mechanical stability and isolation of reactants within unusually shaped and/or flexible batteries.

Conclusion

Through formulation and manual cell fabrication and testing experiments, we have achieved zinc anode, cathode catalyst, and separator materials with two key performance

Figure 9 (a) Freeform-fabricated two-cell zinc-air battery with unusual geometry; (b) partial functionality is retained while the battery is deformed



improvements relative to the material set employed in our initial work:

- 1 in consistent and stable rheology, which allows reliable deposition; and
- 2 in electrochemical activity – as demonstrated by service lifetimes measured in days (as opposed to seconds), and reliable power output of several milliwatts.

Using these materials, the improved fabrication system hardware, and the “backfill deposition” extension to our system software, we have produced several cylindrical batteries with a range of active surface areas. These have been tested under fairly demanding continuous discharge conditions along with several sizes of commercially produced Zn-air button batteries. The data have been analyzed in light of the insights which can be derived from the numerical model of Mao and White (1992), and are presented as a performance benchmark in the field of freeform fabrication of macroscopic batteries. We have also produced and tested a flexible, two-cell battery with an unusual shape that is suggestive of the type of geometric and functional customization that freeform fabrication may bring to the manufacture of batteries.

While our freeform-fabricated batteries have roughly 10 per cent of the energy density and power density of commercially produced batteries, our analysis has suggested possible causes for this – including electrolyte solvent loss, high-internal (possibly contact) resistance, and poor catalyst activity. We will investigate these issues and seek performance improvements in future work. We believe that if we can produce batteries with energy density and/or power density performance within 20 per cent of that of commercially produced batteries, the design freedom afforded by our process will make freeform-fabricated batteries competitive with commercially produced batteries for customized and highly constrained products, including biomimetic robotics, unmanned aerial vehicles, wearable devices, and new and unforeseen applications as well.

References

- Akashi, H. and Tanaka, K. *et al.*, (2002), “A flexible Li polymer primary cell with a novel gel electrolyte based on poly(acrylonitrile)”, *Journal of Power Sources*, Vol. 104 No. 2, p. 241.
- Arcaute, K. and Mann, B.K. *et al.*, (2006), “Stereolithography of three-dimensional bioactive poly(ethylene glycol) constructs with encapsulated cells”, *Annals of Biomedical Engineering*, Vol. 34 No. 9, p. 1429.
- Arnold, C.B. and Kim, H. *et al.*, (2004), “Laser direct write of planar alkaline microbatteries”, *Applied Physics A (Materials Science Processing)*, Vol. A79 No. 3, p. 417.
- Auyeung, R.C.Y. and Wu, H.D. *et al.* (2000), “Matrix assisted laser transfer of electronic materials for direct write applications”, *Proceedings of Society of Photo-optical Instrumentation Engineers, Bellingham, WA, USA*.
- Bahary, W.S. (1984), “Cell gelling agent”, United States Patent 4,563,404, Duracell Inc., Bethel, CT.
- Bates, J.B. and Dudney, N.J. *et al.* (2000), *Thin-film Lithium and Lithium-ion Batteries*, Elsevier, Halkidiki.
- Bennett, P.S. and Kenyon, K.H. *et al.* (1996), “Gelling agent for alkaline electrochemical cells”, United States Patent 5,686,204, Rayovac Corporation, Madison, WI.
- Bidoki, S.M. and Lewis, D.M. *et al.*, (2007), “Ink-jet fabrication of electronic components”, *Journal of Micromechanics and Microengineering*, Vol. 17 No. 5, p. 967.
- Borbely, A. and Molla, J. (1990), “Cathode for zinc air cells”, United States Patent 4,894,296, Duracell, Inc., Bethel, CT.
- Chang, H. and Chi, I. (2001), “Battery and method of making the same”, United States Patent 6,593,023, The Gillette Company, Boston, MA.
- Chen, B. and Cui, T. *et al.*, (2003), “All-polymer RC filter circuits fabricated with inkjet printing technology”, *Solid-state Electronics*, Vol. 47 No. 5, p. 841.
- Chrisey, D.B. and Pique, A. *et al.* (2000), *Direct Writing of Conformal Mesoscopic Electronic Devices by MAPLE DW*, Elsevier, Strasbourg.
- Cohen, D.L. and Malone, E. *et al.*, (2006), “Direct freeform fabrication of seeded hydrogels in arbitrary geometries”, *Tissue Engineering*, Vol. 12 No. 5, p. 1325.
- Corrosion Doctors (2008), “Zn air cell”, available at: www.corrosion-doctors.org/PrimBatt/zinc-air-fig.htm (accessed 16 January 2008)
- Durkot, R.E. and Lin, L. *et al.* (1997), “Zinc electrode particle form”, United States Patent 6,284,410, Duracell Inc., Bethel, CT.
- Fuller, S.B. and Wilhelm, E.J. *et al.*, (2002), “Ink-jet printed nanoparticle microelectromechanical systems”, *Journal of Microelectromechanical Systems*, Vol. 11 No. 1, pp. 54–60.
- Graham, T.O. and Goodman, J.T. (1980), “Electrochemical cells having a gelled anode-electrolyte mixture”, United States Patent 4,681,698, Duracell Inc., Bethel, CT.
- Havener, R. and Boyea, J. *et al.* (2007), “Freeform fabrication of organic electrochemical transistors”, *Proceedings of the 18th Solid Freeform Fabrication Symposium, Austin, TX, USA*.
- Kerg, C.A. (1980), “Alkaline-MnO₂ cell having a zinc powder-gel anode containing starch graft copolymer”, United States Patent 4,260,669, Union Carbide Corporation, Houston, TX.
- Kumar, P. and Das, S. (2004), “Fabrication of meso- and micro-structured devices by direct-write deposition and laser processing of dry fine powders”, paper presented at American Society of Mechanical Engineers, New York, NY.
- Kumar, P. and Santosa, J.K. *et al.*, (2004), “Direct-write deposition of fine powders through miniature hopper-nozzles for multi-material solid freeform fabrication”, *Rapid Prototyping Journal*, Vol. 10 No. 1, p. 14.
- Lianchan, S. and Shaw, L.L. (1999), “Solid freeform fabrication of *in situ* SiC/C thermocouples in macrocomponents”, *Metallurgical and Materials Transactions A (Physical Metallurgy and Materials Science)*, Vol. 30A No. 9, p. 2549.
- Linden, D. and Reddy, T.B. (Eds) (2002), *Handbook of Batteries*, McGraw-Hill, New York, NY.
- Lipson, H. (2005), “Homemade (fabrication technology)”, *IEEE Spectrum*, Vol. 42 No. 5, p. 24.
- Lipson, H. and Pollack, J.B. (2000), “Automatic design and manufacture of robotic lifeforms”, *Nature*, Vol. 406 No. 6799, p. 974.
- Malone, E. and Lipson, H. (2004), “Solid freeform fabrication for autonomous manufacturing of complete mobile robots”, *Proceedings of the Robosphere 2004, Mountain View, CA, USA*.

- Malone, E. and Lipson, H. (2006), "Freeform fabrication of ionomeric polymer-metal composite actuators", *Rapid Prototyping Journal*, Vol. 12 No. 5, p. 244.
- Malone, E. and Rasa, K. *et al.*, (2004), "Freeform fabrication of zinc-air batteries and electromechanical assemblies", *Rapid Prototyping Journal*, Vol. 10 No. 1, pp. 58-69.
- Mao, Z. and White, R.E. (1992), "Mathematical modeling of a primary zinc/air battery", *Journal of the Electrochemical Society*, Vol. 139 No. 4, p. 1105.
- Mironov, V. and Boland, T. *et al.*, (2003), "Organ printing: computer-aided jet-based 3D tissue engineering", *Trends in Biotechnology*, Vol. 21 No. 4, pp. 157-61.
- Mosher, T.J. and Stucker, B. (2004), "Responsive space requires responsive manufacturing-Part II", paper presented at American Institute of Aeronautics and Astronautics, Reston, VA.
- Neudecker, B.J. and Zuhr, R.A. *et al.*, (1999), "Lithium silicon tin oxynitride (Li₂Si₂ON): high-performance anode in thin-film lithium-ion batteries for microelectronics", *Journal of Power Sources*, Vol. 81, p. 27.
- Norteman, W.E. (1978), "Alkaline-MnO₂ sub.2 cell having a zinc powder-gel anode containing P-N-V-P or PMA", United States Patent 4,175,052, Union Carbide Corporation, Houston, TX.
- Oyama, A. and Odahara, T. *et al.* (2002), "Process for producing zinc or zinc alloy powder for battery", United States Patent, 6,746,509, Mitsui Mining & Smelting Company, Ltd, Tokyo, JP.
- Palmer, J.A. and Jokiel, B. *et al.*, (2006), "Mesoscale RF relay enabled by integrated rapid manufacturing", *Rapid Prototyping Journal*, Vol. 12 No. 3, p. 148.
- Passaniti, J.L. and Dopp, R.B. (1994), "Metal-air cathode and cell having catalytically active manganese compounds of valence state +2", United States Patent 5,308,711, Rayovac Corporation, Madison, WI.
- Paul, K.E. and Wong, W.S. *et al.*, (2003), "Additive jet printing of polymer thin-film transistors", *Applied Physics Letters*, Vol. 83 No. 10, p. 2070.
- Pique, A. and Ollinger, M. *et al.*, (2006), "Laser printing of nanocomposite solid-state electrolyte membranes for Li micro-batteries", *Applied Surface Science*, Vol. 252 No. 23, p. 8212.

- PowerPaper Ltd (2005), "Battery specifications", available at: www.powerpaper.com/3_technology/batteryspecs.htm (accessed 15 July 2005).
- Renata, S. (2005), "Hearing aid batteries, product overview", available at: www.renata.com/content/hearingaid/overview.php (accessed 2 October 2007).
- Sumiya, T. and Koike, M. *et al.* (2001), "Gelating agent for alkaline cell and alkaline cell", United States Patent 6,667,133, Sanyo Chemical Industries, Ltd, Kyoto.
- Treger, J. and Sargeant, S. *et al.* (2000), "Alkaline cell with cathode surface protector", United States Patent 6,514,637, The Gillette Company, Boston, MA.
- Urry, L.F. (1998), "Method for producing an electrode containing electrolyte-absorbed polymer particles", United States Patent 6,280,877, Eveready Battery Company, Inc., St Louis, MO.
- Wang, J. and Shaw, L.L. *et al.*, (2004), "Multi-material extrusion for fabrication of artificial teeth", *JOM*, Vol. 56 No. 11, p. 107.
- Wartena, R. and Curtright, A.E. *et al.*, (2004), "Li-ion microbatteries generated by a laser direct-write method", *Journal of Power Sources*, Vol. 126 Nos 1/2, p. 193.
- Weiss, L.E. and Prinz, F.B. (1998), "Novel applications and implementations of shape deposition manufacturing", *Naval Research Reviews*, Vol. 3, pp. 19-26.
- Weiss, L.E. and Merz, R. *et al.*, (1997), "Shape deposition manufacturing of heterogeneous structures", *Journal of Manufacturing Systems*, Vol. 16 No. 4, pp. 239-49.
- West, W.C. and Whitacre, J.F. *et al.*, (2002), "Fabrication and testing of all solid-state microscale lithium batteries for microspacecraft applications", *Journal of Micromechanics and Microengineering*, Vol. 12 No. 1, p. 58.
- Wu, P.K. and Ringeisen, B.R. *et al.*, (2003), "Laser transfer of biomaterials: matrix-assisted pulsed laser evaporation (MAPLE) and MAPLE direct write", *Review of Scientific Instruments*, Vol. 74 No. 4, p. 2546.

Corresponding author

Evan Malone can be contacted at: evan.malone@cornell.edu